HeliNOVI: Current Vibration Research Activities

O. Dieterich
ECD
Ottobrunn
Germany

H.-J. Langer
O. Schneider
DLR
Braunschweig
Germany

G. Imbert
EC
Marignane
France

M.H.L. Hounjet
NLR
Amsterdam
The Netherlands

V. Riziotis
NTUA
Athens
Greece

I. Cafarelli
ONERA
Paris
France

R. Calvo Alonso
SENER
Bilbao
Spain

C. Clerc
VIBRATEC
Ecully
France

K. Pengel
DNW
Marknesse
The Netherlands

Abstract

Reliable vibration prediction for helicopters is still an ambitious task for the rotorcraft community. Current theoretical approaches partition the vibration prediction problem into a vibration excitation task dominated by the main rotor as major excitation source and into a response problem of the elastic airframe. For the analysis of vibratory rotor loads introduced into the airframe, rotor codes considering elastic blades and complex wake structures are state-of-the-art for vibration prediction.

Due to the difficulties experienced in reliable vibration prediction, full scale flight tests are in past and at present a typical approach in industry for the evaluation of rotorcraft vibration behaviour. In order to improve this situation with respect to vibration prediction and reduction, one work package of the European research project HeliNOVI is dedicated to vibration research focussing on a BO105 helicopter by experimental and theoretical means.

The experimental part of HeliNOVI vibration research is based on a wind tunnel test campaign of the BO105 model in the open test section of DNW LLF. The test campaign focussed on the role of the main rotor as most important excitation source for vibrations using advanced measurement techniques like SPR (stereo pattern recognition) and PIV (particle image velocimetry). The wind tunnel test activities are complemented by flight tests of the DLR BO105. These experimental results serve as a comprehensive database for validation purposes of vibration prediction codes within HeliNOVI.

This paper gives an overview of the vibration research activities within the HeliNOVI project. Main focus is given to the preparation and performance of the wind tunnel test campaign and to the presentation of selected wind tunnel test results.

Introduction

Although high vibrations are not directly linked to the flight performance of rotorcrafts, their appearance has manifold drawbacks with respect to operational aspects. On the one hand the rotorcraft requires increased maintenance resulting in additional costs due to fatigue; on the other hand, comfort and health of the crew and the passengers are significantly affected e.g. for EMS services. Therefore, rotorcraft industry is highly interested to have access to adequate tools for solving the complex vibration prediction problem of helicopters. In the past several research and industrial activities were performed to improve the vibration prediction methods culminating into two international workshops for vibratory rotor load predictions in 1974 and 1988 (Refs.1, 2). Nevertheless, the challenging objective of reducing cabin vibrations below a limit of 0.05 g – considered to be adequate for ‘jet smooth ride’ comfort – asks for improved accuracy and reliability of the vibration prediction codes. Furthermore, the tendency of increasing the number of main rotor blades for future helicopters intensifies the requirements for the codes due to the increase of the blade number passage frequency and reduction of blade spacing.

In contrast to fixed wing aircraft, rotorcrafts suffer from several inherent vibration excitation sources. Regarding conventional helicopter configurations, the dominating vibration source is the main rotor and its unsteady aerodynamic environment. In the low speed regime, blade vortex interactions – generated by blade tip vortices of preceding blades passing in the vicinity – typically lead to a significant excitation of the rotor blades resulting in high vibratory hub loads, see Fig.1. A similar

phenomenon is often observed in manoeuvre flight, too.

If the helicopter accelerates in level flight, the convection of the blade tip vortices off the rotor disk plane increases with the consequence of decreasing vibrations as the effects of blade vortex interactions are significantly reduced. In the high speed regime, vibrations are high again, this time due to the increasing influence of asymmetric flow conditions culminating in compressibility effects on the advancing side and dynamic stall effects on the retreating side.

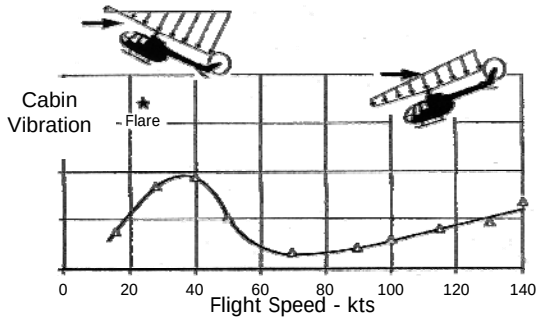

Figure 1: Typical vibration behaviour for level flight and flare

The adequate treatment of all these physical effects is the prerequisite for successful vibration prediction. Although advanced theoretical models exist for several of these aspects, vibration predictions often struggle to fulfil required accuracy levels for the determination of vibratory loads, leaving room for uncertainties in the interpretation of dynamic results during the helicopter development process. Thus, the full vibration reduction potential offered by advantageous rotor and airframe design can not be exploited at the moment by industry due to the shortcomings of current vibration prediction technology. Furthermore, it is difficult to define vibration prediction guidelines in the sense of best practice aiming on improved vibration modelling procedures.

In order to highlight the special challenges posed to vibration prediction tools, it should be kept in mind that the tools aim on calculating small vibratory loads compared to large static values thus asking for high accuracy and robustness of numerical procedures. Furthermore, due to the transformation of loads from rotating into non-rotating frames, accuracy requirements are not only related to magnitudes but also to phase information of the harmonics.

Therefore the validation of vibration prediction tools proved to be a difficult task. Due to the pronounced coupling of structural dynamics and aerodynamics, it is often difficult to identify the components of the theoretical models which require improvements. Experimental results – typically available for validation purposes – consist in strain measurements and accelerations only. In order to overcome these limitations, the HeliNOVI vibration research activities comprise wind tunnel tests with an adequately scaled BO105 model including the measurement of main rotor blade motions by SPR (stereo pattern recognition) and main rotor inflow velocities by PIV (particle image velocimetry). Corresponding to the full scale BO105, the wind tunnel model features a four bladed hingeless main rotor system of type Bölkow and a teetering tail rotor.

In order to close the gap between wind tunnel measurements and full scale applications, a BO105 flight test programme dedicated to HeliNOVI vibration research was performed by DLR.

This paper gives an overview of the HeliNOVI vibration research activities both on experimental and theoretical side. Main focus is given to the preparation and performance of the wind tunnel test campaign and to the presentation of selected wind tunnel test results.

Objectives

The HeliNOVI project addresses the following two topics linked together by a common wind tunnel test campaign:

- Helicopter vibration reduction
- Tail rotor noise reduction

For an overview of the overall HeliNOVI project the reader is referred to Ref.3 while for details with respect to HeliNOVI tail rotor noise activities, information is given in Ref.4 and Ref.5. This paper focuses on the vibration research activities within HeliNOVI.

The key topics within the vibration part of the HeliNOVI project are:

Wind tunnel testing
Wind tunnel test results of a scaled helicopter model will be analysed in detail for tool validation purposes. Wind tunnel testing is aimed at the validation of design codes and modelling techniques for vibration prediction. Testing of the complete wind tunnel model including fuselage and tail rotor allows qualifying and quantifying interactional aero-dynamic effects on vibratory loads.

Vibration excitation sources
The results of the wind tunnel tests and complementary theoretical investigations will

be used for the identification and assessment of vibration excitation sources. These activities will improve the physical understanding of rotor induced vibrations in the complex aerodynamic environment of main rotor, fuselage, empennage and tail rotor.

Full scale flight testing
Full scale flight test results will be compared to the wind tunnel test data of the scaled model and related theoretical results. Objective is the assessment of wind tunnel test results with respect to full scale and free flight conditions. Focus will be given to the transferability of the vibratory response behaviour from model to full scale.

Design guidelines
Based on the improved understanding of the aerodynamic and dynamic phenomena, means for vibration reduction with emphasis on interactional aerodynamics will be analysed and evaluated leading to design guidelines for future low vibration helicopters.

HeliNOVI Flight Test Campaign

DLR performed a flight test campaign using a BO105 helicopter (see Fig.2) in order to establish a complementary full scale database for HeliNOVI. The serially installed blade flap absorbers of the helicopter were removed in order to match the wind tunnel model configuration with respect to vibratory loads. Furthermore, supplementary strain gauge sensors and accelerometers were mounted at the rotor hub for a sensor equipment comparable to the wind tunnel model. The test helicopter was additionally equipped with a special low airspeed sensor system called LASSIE for accurate measurement of low flight speeds.

The flight test programme consisted mainly of level flight test points as these operating conditions are typically of most relevance for comfort due to their large share on the overall flight time. Beside flight speed the test points differ by helicopter gross weight (minimum operational TOW versus maximum TOW) and pilot trim (bank angle versus side slip).

Planning of Wind Tunnel Campaign

Measuring vibratory wind tunnel model hub loads has always posed significant challenges to experimental techniques. Due to the encountered difficulties with respect to sensing small dynamic loads in the presence of large static forces and moments, the dynamic load components are typically suspicious to major uncertainties. These shortcomings are one of the major reasons for only limited wind tunnel test activities dedicated to vibratory hub load measurements in the world. Publications demonstrating the high technical demands for adequate vibratory hub load measurements are given in Ref.6 and Ref.7 for example.

Figure 2: BO105 operated by DLR

Therefore, test data available at the beginning of the HeliNOVI project from earlier flight and wind tunnel[i] test campaigns were analysed and compared with special focus on higher harmonic signals. The results recommend the usage of strain gauges as reliable load sensors while the balance systems i.e. rotor balance and fuselage balance can not be applied straight forward. This conclusion is in line with the experience gained from other test campaigns e.g. investigated by ONERA and EC. Therefore, comprehensive activities were started within HeliNOVI by DLR and VIBRATEC in order to analyse the applicability of dynamic calibration with respect to the rotor balance.

Regarding strain gauge measurements, Fig.3 shows the correlation of 3/rev flap bending moment amplitudes[ii] at 33% span station. In contrast, the comparison of 4/rev lead-lag moments, see Fig.4, shows deviations in order of one magnitude explained by the differences in the drive train system dynamics thereby underlining the general need of appropriate drive train system modelling for accurate vibration prediction.

For adequate comparisons between wind tunnel model and full scale BO105, special attention was given to the appropriate definition of model trim parameters and values including the application of wind tunnel corrections (Ref.8). Focusing on vibratory loads, primary objective is a comparable loading of the main rotor.

[i] BO105 model without tail rotor system
[ii] BO105 flight test results downscaled

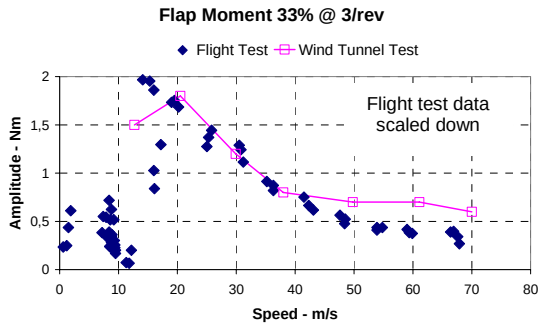

Figure 3: 3/rev flap bending moments

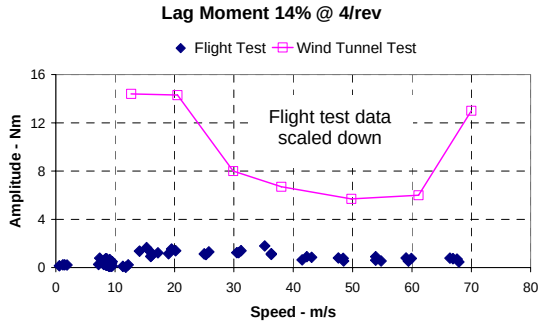

Figure 4: 4/rev lag bending moments

Compared to flight tests, the wind tunnel test campaign offers the possibility to easily study design variants of the envisaged helicopter. Regarding the full helicopter configuration of the BO105 model, interactional aerodynamic effects are expected to appear due to the presence of the fuselage and the tail rotor. Modifications with respect to fuselage and tail rotor should help to identify and validate these interactional effects. As the noise research part of HeliNOVI concentrates on the tail rotor, tail rotor modifications of the wind tunnel model are defined with respect to the special needs of noise investigation e.g. change of tail rotor sense of rotation, change of tail rotor location, see Ref.5. Regarding the fuselage interacting with main rotor inflow, the distance between main rotor hub and fuselage is identified as primary parameter. Because it is impossible to change rotor shaft length of the wind tunnel model within this project, another approach was chosen in order to simulate hub-fuselage distance changes. As presented in Fig.5, the fuselage of the model was modified with a large top fairing geometrically obtained by a shift of the upper fuselage surface in shaft direction, see Fig.6.

Performance of Wind Tunnel Tests

The wind tunnel test campaign for the vibration research activities took place end of August 2004 in the DNW LLF[iii]. As the campaign was dedicated to noise and vibration measurements, the natural choice for the wind tunnel configuration was the open test section due to aero-acoustic testing requirements.

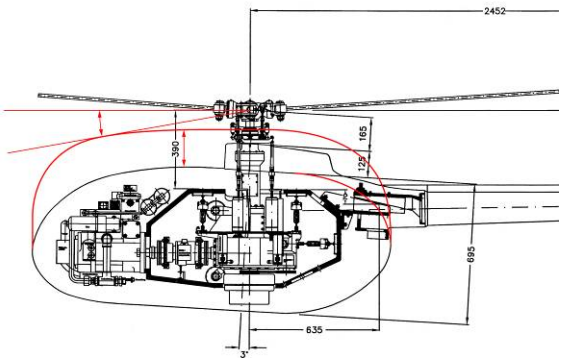

Figure 5: Modified fuselage contour

Figure 6: Model with modified fuselage contour

Besides loads and accelerations measured by the wind tunnel model sensors for all test points, the vibration test campaign comprised additionally SPR (stereo pattern recognition) and PIV (particle image velocimetry) measurements for selected cases. The objectives of the SPR measurements are the evaluation of higher harmonic blade motions for code validation purposes and the support of the PIV measurement campaign by the determination of blade positions in the wind tunnel frame. The performance of the SPR test and SPR data processing is in general similar to former test campaigns (Ref.9).

The objectives of the PIV measurements are the observation of flow characteristics (inflow velocities) in the vicinity of the main rotor and the evaluation of wake structures for validation of the free wake codes. For these purposes, special attention was given to the PIV window set-up and sampling procedures. Fig.7 shows the principal arrangement of the PIV windows in a sketch. The PIV windows are arranged vertically in order to use the same set-up for

[iii] Large-Low speed Facility

main rotor and tail rotor PIV measurements. Due to an equidistant lateral spacing of 200 mm, the number of PIV windows amounts to approximately 50 on both advancing and retreating side. Due to shadowing by the fuselage, the selection of PIV windows in the immediate vicinity of the fuselage is not recommended.

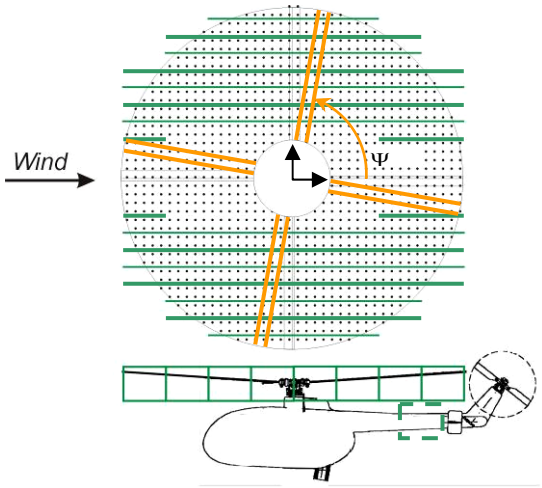

Figure 7: Nominal PIV window arrangement

For each PIV window 48 images were shot with a spacing of 11.25 deg by special triggering procedures. This approach results in a low number of images with the same nominal blade azimuth (six images if identical blade behaviour is assumed). This is in contrast to "conventional" PIV measurements (e.g. Ref.10) where averaging is performed over a large number of images for improving data reliability.

Three flight states were analysed by both SPR and PIV. In order to select test points which are representative for vibration the following wind speeds were chosen for level flight conditions:

- 12 m/s: This test case is characterised by high vibrations due to pronounced blade vortex interactions.
- 50 m/s: Due to the reduced influence of blade vortex interactions, this test case is in the vicinity of the vibration minimum in forward flight.
- 70 m/s: This test case is chosen as it defines the maximum wind speed achieved during the wind tunnel test campaign.

Additional test points with wind speeds between 12 m/s and 70 m/s were measured regarding vibratory loads and accelerations for the baseline wind tunnel model, model configurations with modified tail rotor and the model configuration with modified fuselage.

Results

The following sub-chapters focus on the experimental results obtained by strain gauges and accelerometers, pressure sensors, SPR and PIV giving an overview of the preliminary outcome of the wind tunnel test campaign.

Theoretical results – compared to the experimental data where appropriate – are presented here for the purposes of checking the validity of the results and identifying areas where models and codes need improvements. The theoretical results are based on aeroelastic models which were established for pre-test predictions by NTUA (using an in-house code) and ECD (using commercial codes).

Strain gauges and accelerometers

Regarding post-processing of wind tunnel test data, ONERA focused on the analysis of strain gauge and accelerometer signals with respect to hub load determination. Hub load data were obtained by means of different kinds of transducers located in the fixed or in the rotating frame:

- Two fixed 6-component main rotor balances located at about 0.39 m below the rotor centre; the first one, referred as the piezo balance, allows only the measurement of dynamic loads whereas the second one, referred as force balance, allows the measurement of the static plus dynamic forces.
- Two rotating accelerometers oriented in flap and lag directions and located on the hub arms of two opposite blades near the rotor centre
- One upper fixed accelerometer positioned near the swash plate and a lower one near the gear box
- Two mast bending gauges attached to the rotating shaft at two sections at 75 mm and 175 mm below the hub centre
- One vertical mast extension gauge
- Four gauges equipping the pitch links of the four-bladed rotor

Finally, local blade data at different radial stations were obtained using flap, lag and torsion blade gauges.

Hub load time data were acquired over 32 revolutions and were also processed as harmonic coefficients (ten harmonics per rotor revolution). Analysis is therefore concentrated on both time signals and harmonic contents. Fig.8 shows this dual analysis applied to a vertical transducer of the main rotor balance

which allows checking the repeatability of the response of the transducer over the 32 revolutions (waterfall plot) and the harmonic content of the averaged signal.

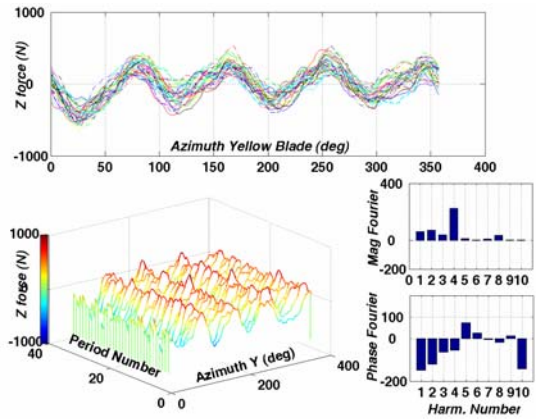

Figure 8: Time history and harmonic analysis of vertical force component

A first analysis of the fixed frame vibratory loads was performed for wind speed sweep ranging from 12 m/s to 70 m/s using the main rotor balance and the rotating mast gauges. It should be noted that in order to check the dynamic loads, a dynamic calibration of the main rotor balance was planned. However, this latter was not fully completed; therefore the static calibration was used instead for the following figures.

On the other hand, the two rotating mast gauges were extended virtually to a four rotating mast gauges balance by shifting the existing gauge signals by 90 deg, converted into loads in the fixed frame and harmonically processed before being compared with the main rotor balance loads, see Fig.9 for the main rotor hub pitch moment.

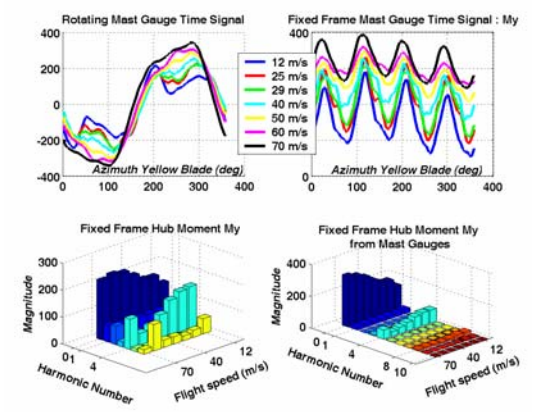

Figure 9: Hub pitch moment measurements versus flight speed – unit Nm

The main rotor vertical hub force was processed using either the extension mast gauge or the vertical cells of the main rotor balance, see Fig.10. Compared to the main rotor balance the extension mast gauge sensor shows a significant amount of noise in the signal.

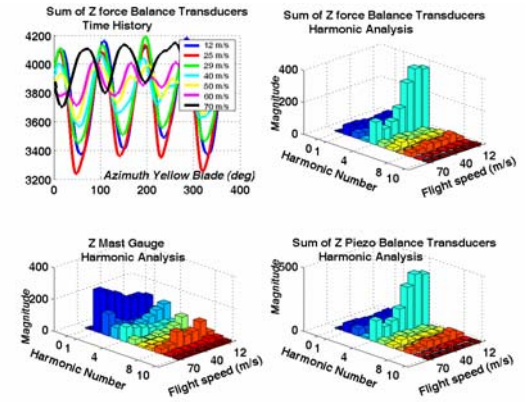

Figure 10: Hub vertical force measurements versus flight speed – unit N

Finally, linear accelerations in all directions were analysed at two mast locations (near the swash plate and near the gearbox). As one can see in Fig.11 for the gearbox sensor, the time signal seems very noisy but once filtered the harmonic components appear to confirm the same trends as those observed with other sensors.

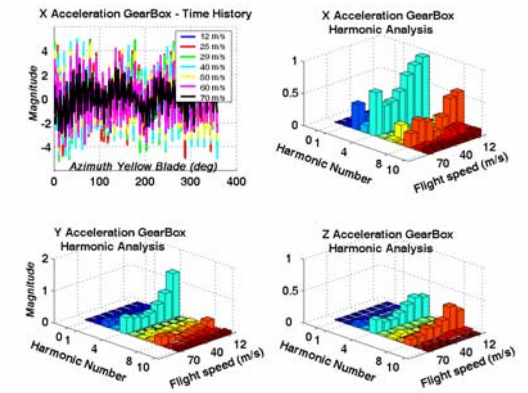

Figure 11: Acceleration measurement gearbox versus flight speed – unit g

All these results lead to the following remarks:

- The highest vibratory levels are encountered for transition and high speed regimes due to blade vortex interactions and compressibility effects. It appears therefore essential to be able to predict accurately the rotor blade loads for these two flight regimes.
- Almost always, the trends observed are similar whatever the experimental processing (direct balance measurement or indirect from mast gauges) or the transducers are taken into account.

- The harmonic content of the fixed frame hub loads is – as expected – mainly dominated by the 4/rev and the 8/rev components.

SENER processed the blade load sensors in a similar way. The following figures present main rotor blade bending moments acting on the rotor hub at 3% radial station for the baseline wind tunnel model and for the model with modified fuselage contour. Only cases with existing test points for the modified wind tunnel fuselage are shown for clarity. Furthermore, the figures incorporate numerical results for comparison reasons. Fig.12 shows the behaviour of 3/rev blade flap moments. This figure demonstrates that the modification of the fuselage affects the blade flap moments especially in the high speed flight regime as expected by theory. Results for 4/rev and 5/rev flap moments – not presented here – show generally a similar behaviour.

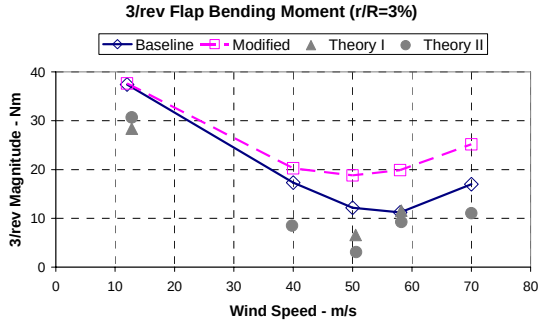

Figure 12: 3/rev blade flap moments

Regarding blade lag moments, the situation is similar to the comparison of wind tunnel model and full scale helicopter already presented in Fig.4. High 4/rev values were measured for the wind tunnel model while the numerical results – neglecting any drive train influence by assuming fixed rotor speed – indicate low amplitudes, see Fig.13.

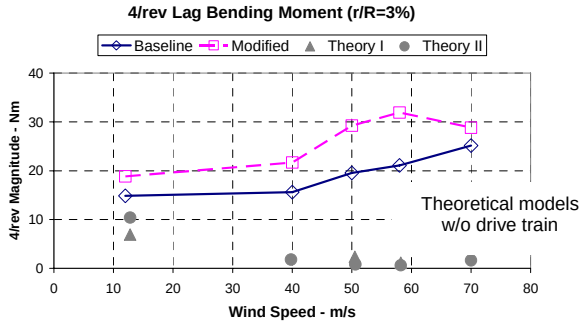

Figure 13: 4/rev blade lag moments

Pressure test data analysis

In the post-processing phase, NLR focused on the detailed analysis of the pressure test results. The measured pressure data mainly consist of instantaneous time traces for all revolutions. The analysis presented here is aimed at the effect of the azimuth on the revolution-averaged aerodynamic pressures. Generally, aerodynamic results are analysed at three different levels:

1-D (t)[iv]: The rotorcraft level, dealing with the global aerodynamic loads on the rotorcraft, its main and tail rotors and interference effects.

Due to the limited number of unsteady pressure sensors on the airframe (Fig.14), the wind tunnel model was only partially suited for a detailed analysis of aerodynamic loads acting on the airframe. To improve this situation the so-called warping technique – introduced in Ref.11 for fluid-structure interactions and applied to analyse pressure distributions in Ref.12 – has been employed in this analysis. With this technique (Ref.13) the pressure data is fully expanded over surface grids modelling the wetted surfaces of the rotorcraft (Fig.15). The warping analysis resembles a digital pressure sensitive paint giving information in a more qualitative manner.

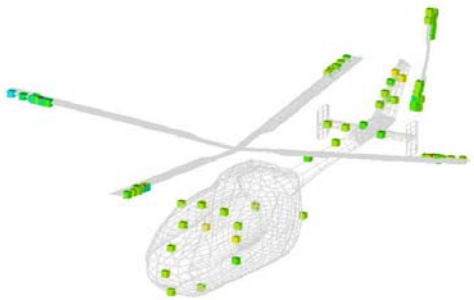

Figure 14: Overview of wind tunnel model unsteady pressure sensor locations

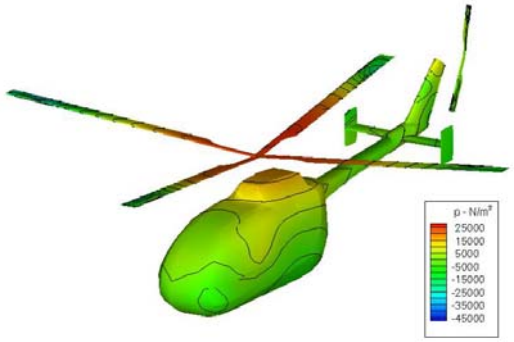

Figure 15: Application of warping technique, wind speed 70 m/s

2-D (r, t)[v]: The blade level, dealing with the local aerodynamic loads over the blades.

Similar to the rotorcraft level, the analysis is complicated by the limited amount of pressure

[iv] Global data depending only on time t
[v] Blade data depending on radius r and time t

sensors as the layout of the aerodynamic sensors was not directed to study these effects in detail.

3-D (c, r, t)[vi]: The sectional or local level, dealing with pressure distributions.

From the many type of data that have been depicted by NLR for visualisation and assessment of the experimental data this paper presents only a small selection of the results with emphasis on the main rotor and on interactional aerodynamics.

Resolution averaged pressure coefficients on the fuselage: As already introduced contours of pressure distributions over the fuselage are obtained by warping from the scarce measured discrete data (26 sensors) to the wetted surfaces of the fuselage by applying AESIM-BASIC's (Ref.11) warping algorithms. The warping allows to track in a qualitative manner the evolution of the aerodynamic pressure waves over the surfaces. Data is depicted in Fig.16 for a wind speed of 70 m/s and rotor azimuth 90 deg for the baseline configuration of the wind tunnel model. Investigations are under way comparing the experimental and theoretical results with special emphasis on the soundness of the pressure sensors on the fuselage.

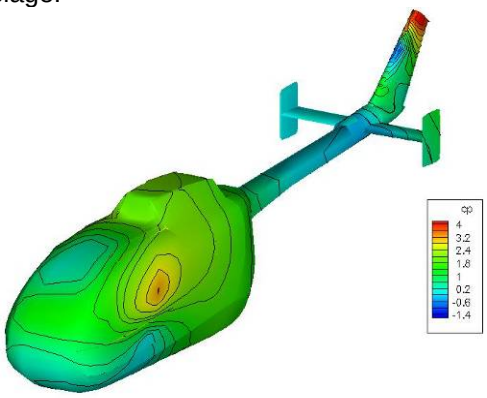

Figure 16: "Warped" pressure distribution, 70 m/s wind speed, azimuth 90 deg

Resolution averaged pressure on the whole configuration: In addition, contours of pressure distributions over the whole configuration are obtained by dynamic warping from the measured data available on the fuselage and the blades to all wetted surfaces of the rotorcraft. While Fig.15 presents the pressure coefficient distribution over the wind tunnel model for a wind speed of 70 m/s, Fig.17 shows the model tail area for selected azimuth angles at the same wind speed clearly indicating an interactional effect on the left fin of the horizontal stabiliser. The applied scales are dominated by the pressures acting on the main rotor.

Normal force coefficients about the quarter chord: Fig.18 presents the chordwise pressure distribution at radial section 87% of the main rotor for a wind speed of 33 m/s including a comparison with theoretical results. The comparison is fairly good. The normal force component at the same section obtained by integration is shown in Fig.19 and Fig.20 for a wind speed of 33 m/s and 59 m/s, respectively.

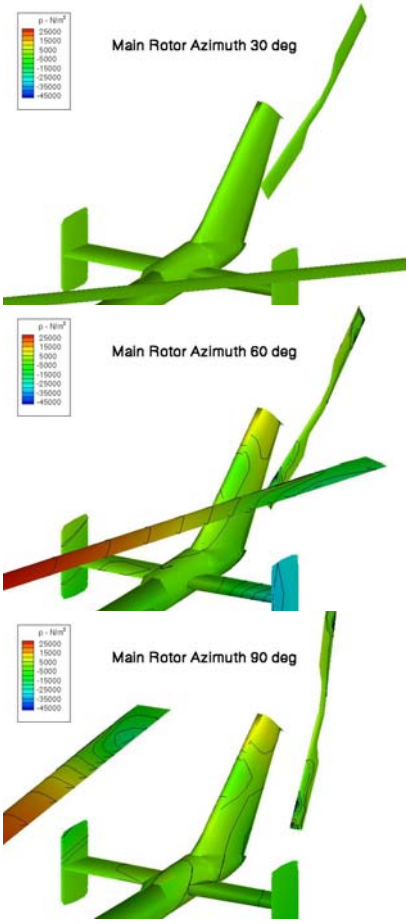

Figure 17: "Warped" pressure distribution, 70 m/s wind speed

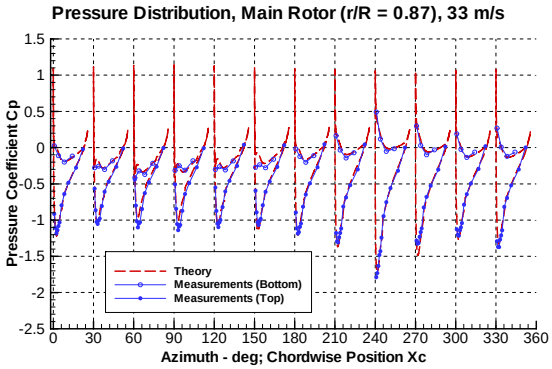

Figure 18: Local pressure coefficients, 33 m/s

[vi] Local data depending on location (c,r), time t

A comparison with theoretical results is made in order to check the aerodynamic loading of the main rotor. The comparison is relatively fair. Besides other reasons, differences between experimental and theoretical results might also be related to the number of pressure sensors in chordwise direction, especially for the lower side.

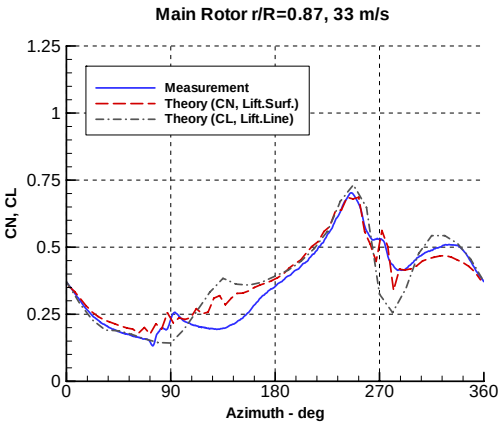

Figure 19: Normal force coefficient, 33 m/s

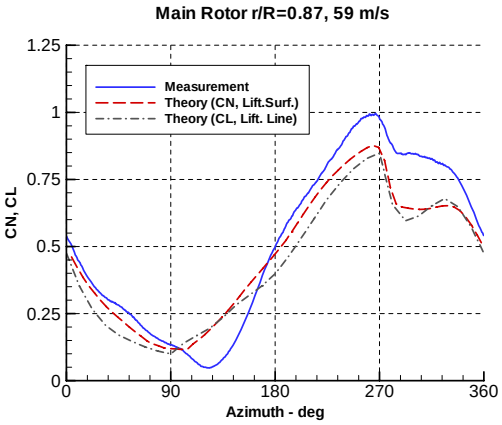

Figure 20: Normal force coefficient, 59 m/s

SPR (Stereo Pattern Recognition)

In the HeliNOVI project, DLR is responsible for processing SPR. The SPR method determines optically the spatial position of markers painted on each of the four blades and on the fuselage by four cameras widely spaced on ground. The technique is based on a 3-dimensional reconstruction of visible marker locations by using stereo camera images. Theoretically, the accuracy of marker position recognition is about 0.4 mm in x-, y- and z-direction. A more detailed description of the method is presented in Ref.14.

Setup: For the SPR measurements two independent camera systems were used. Each camera system contains two cameras which are mounted on the ground of the wind tunnel hall in order to have a fixed orientation among each other. The cameras are located in front and in the back of the model focused on the advancing and the retreating side of the rotor disk such that the entire disk is observed by a single test run. For calibration of the SPR system special reflective markers were taped on all blades and were localized by means of Theodolites.

For the HeliNOVI test campaign, a total of 36 white markers (called blade marker) were painted on the lower side of each rotor blade (Fig.21). These markers were distributed equally all along the leading and trailing edge such that 18 radial stations were covered from radius r/R=0.23 to 0.994. Additionally, for purposes of hub centre localization and drift compensation three markers were attached underneath the fuselage shell (lower body markers) and two markers on each side of the shell (body markers). The SPR measurements were performed with azimuth increments of 11.25 deg respectively 32 azimuth positions per revolution such that the analysis allows to synthesize the lower harmonics from the time history of the blade motion. On each azimuth position 50 images were taken for averaging to get smooth data.

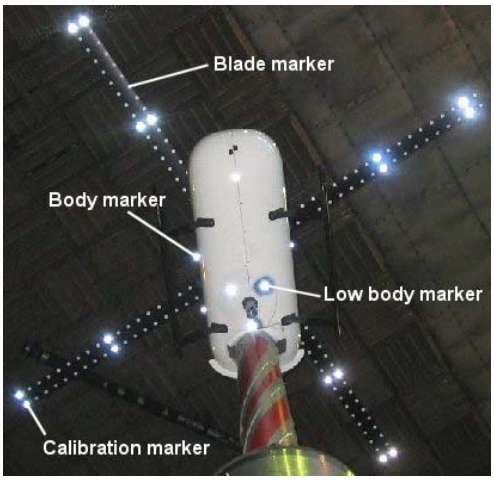

Figure 21: Marker setup HeliNOVI

Preparation of raw data: In a pre-processing step DNW evaluated the camera images resulting in x-, y- and z-positions of the markers along leading and trailing edge in space, i.e. in the wind tunnel coordinate system. The SPR measurements are aimed on flap, lead-lag and torsion displacements of the quarter chord line in the shaft coordinate system with origin in the centre of the rotor hub. To eliminate fluctuations a mean value of all 50 images is computed. The peak to peak scattering is less than 5 mm in z-direction and by about 45 mm in tangential direction (y-direction in Fig.22 for blade azimuth 0 deg) due to an azimuth instability caused by a defective 1/rev trigger signal.

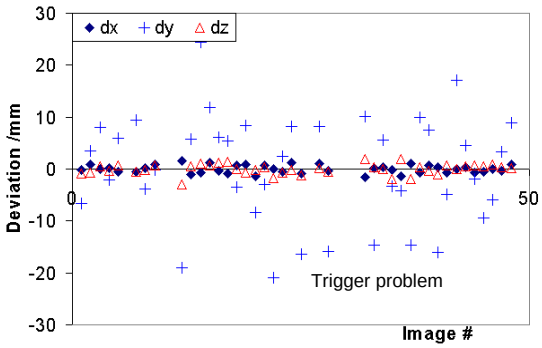

Figure 22: Scattering of blade marker #39 at azimuth 0 deg

For calculation of the blade deflection and blade motion parameters the rotor hub centre location must be known for the transformation of the blade and body marker coordinates from the wind tunnel system to the rotor hub centre system. The position of the hub centre could not be directly measured since the camera view is from below. To localize the centre position in the rotor plane (x-y-direction) a circular regression is applied after transforming all data by the shaft pitch and roll angle. More details are presented in Ref.9. Assuming that each single blade marker travels along a circle around the hub centre a best fit is calculated whereby the obtained centre point of the circle is related to the centre position of the rotor (Fig.23). Thus there are 36 centre points per blade for 36 blade markers. The comparison of the results show a variation of less than 0.5 mm in x-y-direction where all computed centre points of all four blades are within (Fig.24).

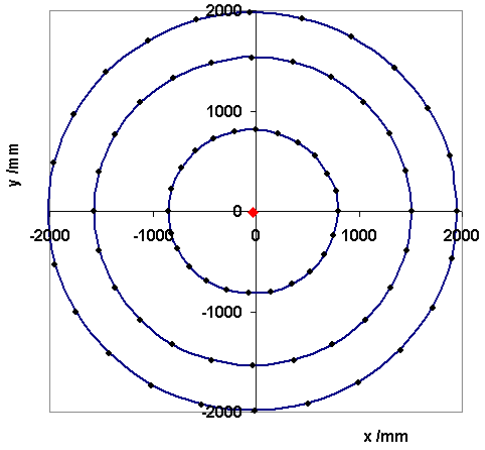

Figure 23: Best fit circles for determination of the rotor hub centre

The vertical hub centre location is obtained by using the fixed body marker. With the known geometry relation between body markers and hub centre the vertical hub centre position is calculated with an error of less than 0.5 mm since the marker recognition accuracy is 0.4 mm. Now the coordinate system is shifted into the rotor hub system and the blade deflections are computed accordingly.

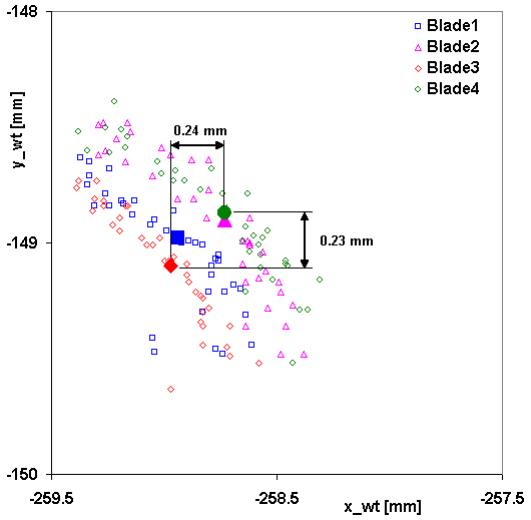

Figure 24: Rotor hub centre position in x-y-direction for 50 m/s case

Blade motion: All blade motions like elastic flap, lead-lag and torsion are related to the quarter chord line of the blade calculated from the leading and trailing edge blade markers by interpolation. For an analytical description of the blade motions, Fourier coefficients up to 5/rev were established for each radial station by a best fit over all azimuths.

The elastic flap deflection (positive up) is obtained by the distance of the actual quarter chord line to a straight line defined by the pre-cone angle of the blade. For the 50 m/s case, Fig.25 presents elastic blade flapping at the blade tip versus azimuth while Fig.26 shows the radial flap distribution for a blade azimuth of 150 deg. It is noticeable that the measured variation between blades has a similar magnitude of order as the comparison between different codes (grey dashed lines).

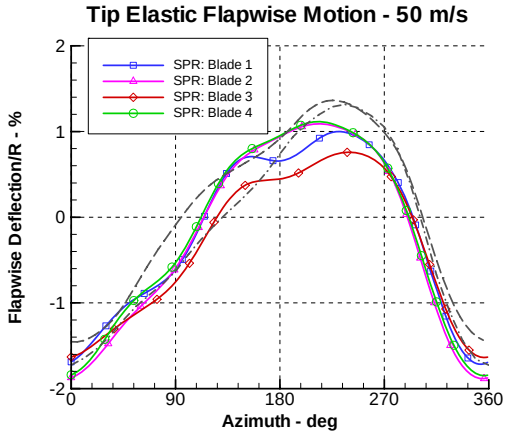

Figure 25 Elastic blade tip flapping motion for 50 m/s (theoretical results – grey dashed lines)

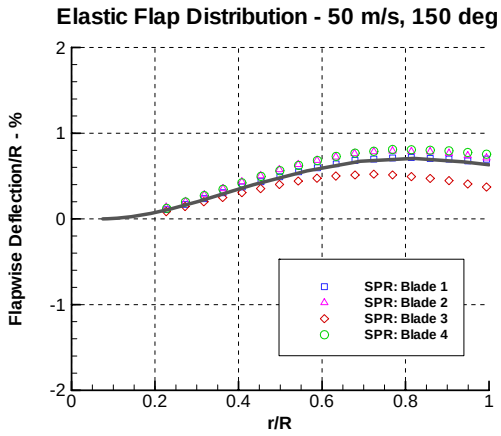

Figure 26: Elastic blade flapping at blade azimuth 150 deg for 50 m/s (theoretical result – grey line)

The elastic blade tip lead-lag deflection (lag positive) is given by the distance between the radial position of the blade quarter chord line and a straight line defined by the current azimuth position of the blade. Results of the blade tip lead-lag displacement versus azimuth are shown in Fig.27 for the 50 m/s case. The significant bias of the experimental values compared to the theoretical results (grey dashed lines) is still under investigation focussing on the time delay of data acquisition and on structural properties of the drive train system.

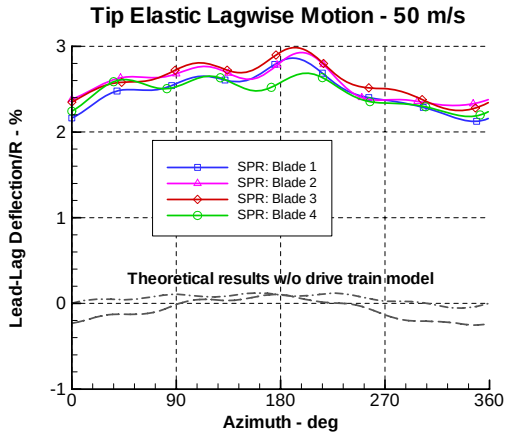

Figure 27: Elastic blade tip lag displacement for 50 m/s (Theoretical results – grey dashed lines)

For the calculation of the elastic blade torsion the vertical position of the leading and trailing edge blade markers is used where the controlled pitch angle, the vertical offset of the blade markers and the linear blade pre-twist have to be subtracted (Fig.28). Theoretically the error in blade torsion is about 0.5 deg, caused by the marker recognition accuracy and the spatial distance of leading and trailing edge markers. Because of this approach there is a significant scattering of the results in radial direction. That is the reason why a regression function is computed for each azimuth position based on the first mode shape of blade torsion. In order to understand the differences between measurements and theoretical results (grey dashed lines), blade pitch in the blade root area was also analysed showing clearly the need for adequate consideration of pitch control flexibility which has to be adjusted in the theoretical models.

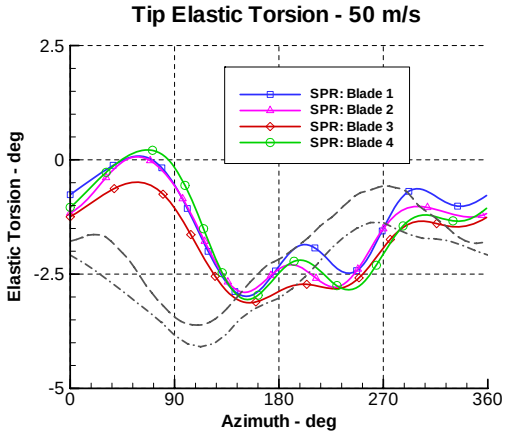

Figure 28: Elastic blade tip torsion for 50 m/s (theoretical results – grey dashed lines)

PIV (Particle Image Velocimetry)

In the vibration part of HeliNOVI, ECD post-processed and analysed PIV data. Up to now PIV – allowing the sensing of flow fields – was especially used for the analysis of vortex structures with respect to rotary wing applications. In contrast the usage of PIV within the vibration part of HeliNOVI mainly aims at the substantiation of main rotor inflow velocities.

The principle of PIV consists in seeding of small particles (e.g. oil) into the flow field of the wind tunnel and in monitoring the motion of these particles by laser pulses. Using two pulses in a short time period allows the calculation of velocity components by comparing the two resulting images and the tracking of the particle motions. For the calculation of all spatial components of the velocity vector, stereoscopic techniques are applied based on the application of two digital cameras under different positions – an approach similar to SPR. Fig.29 shows the PIV test set-up for the main rotor retreating side. For the advancing side (Fig.30), the common support frame – carrying the laser and the digital cameras – is rotated to the other wind tunnel model side thus avoiding the need for an additional calibration run.

Regarding the PIV observation windows the size of each window was given by 1280 pixels by 1152 pixels. Based on a resolution of

3.3 pixels/mm a PIV observation window spans over 0.388 m by 0.349 m. DNW provided PIV results based on two different interrogation areas with varying size. The interrogation areas are selected to 64x64 pixels and 32x32 pixels. For investigations of the inflow characteristics, 64x64 pixels are the adequate choice. The interrogation areas are overlapped by 50% in both directions as shown in Fig.31. The velocity vectors are derived for the centroids of the interrogation areas.

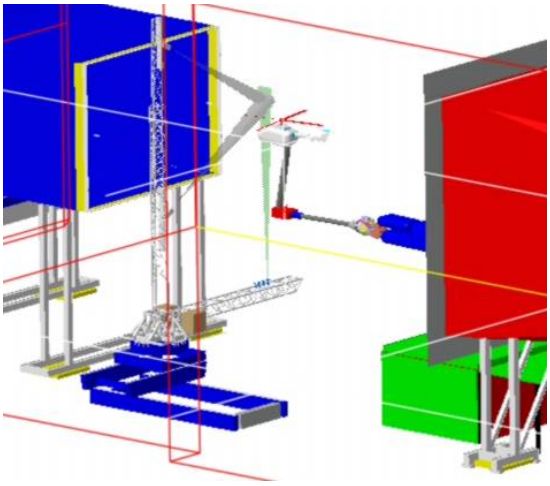

Figure 29: PIV set-up main rotor retreating side

Figure 30: PIV measurements advancing side

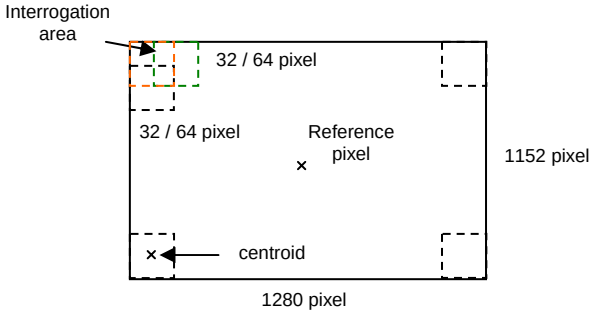

Figure 31: PIV observation window

Based on the wind tunnel coordinates of the reference pixel and of the rotor hub centre, the location of the PIV observation window with respect to the main rotor hub centre is derived in the wind tunnel coordinate system.

For the validation of aeroelastic codes – especially in the field of inflow modelling – the velocity vectors in the vicinity of the main rotor disk plane are of high interest for comparison reasons. In order to derive these vectors for the rotor disk plane, two steps are required; first to establish the rotor disk plane in the wind tunnel coordinate system; second to map the flowfield information onto the intersection of rotor disk plane and PIV observation area. By this procedure, the huge amount of PIV data is reduced by one dimension. A natural approach to establish the rotor disk plane in the wind tunnel coordinate system is the usage of SPR data. As the processing of SPR data was still under way, an alternative procedure was chosen. For the PIV data reduction presented here, theoretical predictions serve as database for the definition of a cone approximating the rotor blade positions by a rigid blade model with artificial hinge offset.

The intersection of the PIV planes with the rotor disk leads to hyperbola curves which typically do not directly match the collocation points of the PIV arrays. Therefore, procedures were evaluated for mapping or interpolating the PIV measurements onto the rotor disk plane. With respect to the usage of the 64x64 pixel data already showing “adequate smoothing” behaviour, the following scheme was selected based on linear interpolation of four collocation points (Fig.32).

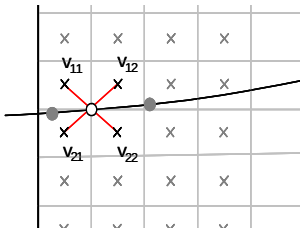

Figure 32: Interpolation scheme

For the 12 m/s case, Fig.33 presents vertical components of the induced velocity at a butt line of 0.843 m on the retreating side for a blade azimuth of 0 deg. While the marker symbols represent data points of the six images the solid line shows the result of “simple” averaging over the images. Two events are clearly visible in the vicinity of $x_{Hub} = –0.8$ m and $x_{Hub} = 0.1$ m. The appearance of the first event is related to a tip vortex in the vicinity of the rotor disk. The

second event is related to the influence of the neighbouring blade at 90 deg azimuth leading to significantly scattered results. In a similar way, Fig.34 shows results for the 50 m/s case at the same azimuth at a butt line of 0.899 m on the retreating side.

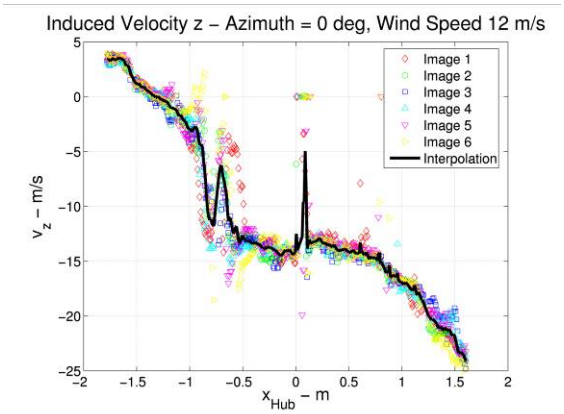

Figure 33: Averaging of images for 12 m/s case (y = –0.843 m)

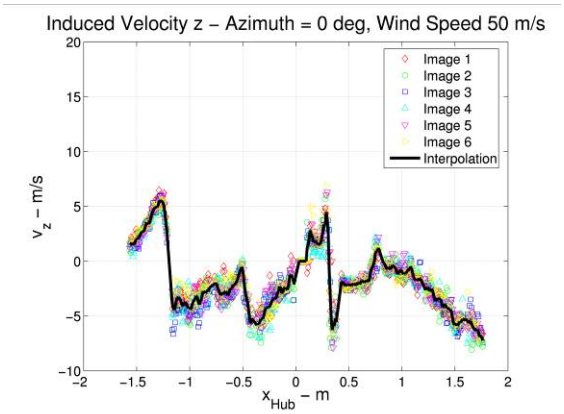

Figure 34: Averaging of images for 50 m/s case (y = –0.899 m)

In Fig.35, the measured induced velocities are compared to calculations for the 12 m/s case. Two theoretical results are presented – with and without inclusion of a fuselage panel model. The agreement between experimental and theoretical results might probably be improved by taking into account the measured azimuth angle instead of the nominal one for averaging. Fig.36 shows experimental and theoretical results for the 50 m/s case – this time the theoretical results comprise only the model with fuselage.

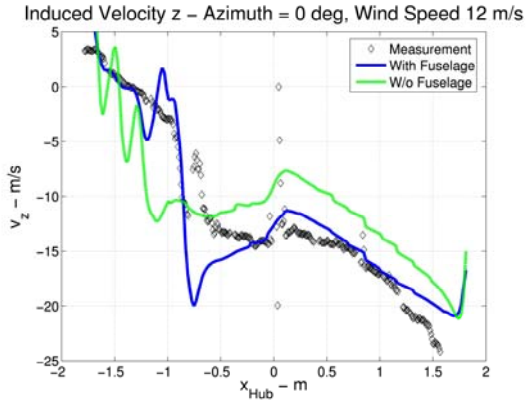

Figure 35: Comparison of induced velocities for 12 m/s case (y = -0.843 m)

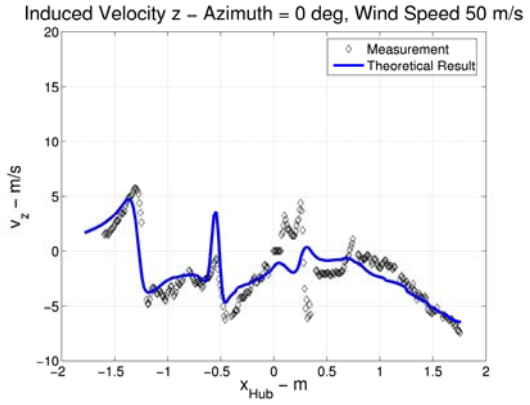

Figure 36: Comparison of induced velocities for 50 m/s case (y = –0.899 m)

Conclusions

This paper presents an overview with respect to the current vibration research activities of the HeliNOVI project.

Studies comparing former wind tunnel test and flight test results of the BO105 have indicated that carefully performed wind tunnel measurements may offer valuable physical insight into the vibration problem with focus on the excitation side. Thus, an important milestone of the HeliNOVI project was the performance of wind tunnel tests of an adequately scaled BO105 wind tunnel model at DNW LLF.

After the wind tunnel test campaign main activities consisted in processing and checking of the experimental data which can be grouped as follows:

- Strain gauge and accelerometer signals
- Pressure sensors on fuselage and rotors
- SPR (stereo pattern recognition) data
- PIV (particle image velocimetry) data

Selected experimental results were shown accompanied by corresponding theoretical results where adequate. The initiated comparison of data intensified the expectation that the wind tunnel tests were successful with respect to the objectives of HeliNOVI. First validation activities indicated encouraging results and identified modelling issues which are expected to enhance the agreement between test and theory. Current and future activities are focused on:

- Detailed comparison with theoretical results and validation of the free wake codes
- Comparison of results with BO105 flight tests performed by DLR for the HeliNOVI project
- Experimental and theoretical analysis of parameters aiming at a reduction of vibratory loads

Acknowledgements

The authors gratefully acknowledge the support of the European Commission for the HeliNOVI project enabling industry, research centres and universities to face the challenging helicopter vibration prediction problem in a cooperative and fruitful manner.

References

Ref.1 *Ormiston, R.A.,* Comparison of Several Methods for Predicting Loads on a Hypothetical Helicopter Rotor, Journal of the American Helicopter Society, 19(4), 1974

Ref.2 *Hansford, R.E., Vorwald, J.,* Dynamic Workshop on Rotor Vibratory Loads Prediction, Journal of the American Helicopter Society, 43(1), 1998

Ref.3 *Langer, H.-J., Dieterich, O., Oerlemans, S., Schneider, O., van der Wall, B., Yin, J.,* The EU HeliNOVI Project – Wind Tunnel Investigations for Noise and Vibration Reduction, 31st European Rotorcraft Forum; Florence, Italy; Sept 13-15, 2005

Ref.4 *Voutsinas, S.G., Arnaud, G., Dummel, A., Falchero, D., Pidd, M., Prospathopoulos J., Visingardi, A., Yin, J.,* Aerodynamic Interference in Full Helicopter Configurations and Assessment of Noise Emission: Pre-test Modelling Activities for the HeliNOVI Experimental Campaign; 31st European Rotorcraft Forum; Florence, Italy; Sept 13-15, 2005

Ref.5 *Yin, J., van der Wall, B., Oerlemans, S., et al,* Representative Test Results from HELINOVI Aeroacoustic Main Rotor/Tail Rotor/Fuselage Test in DNW; 31st European Rotorcraft Forum; Florence, Italy; Sept. 13-15, 2005

Ref.6 *Gabel, R., Sheffler, M., Tarzanin, F.J., Hodder, D.,* Wind Tunnel Modeling of Rotor Vibratory Loads, American Helicopter Society 38th Annual Forum, Anaheim, California, May 1982

Ref.7 *Staley, J.A., Mathew, M.B., Tarzanin, F.J.,* Wind Tunnel Modeling of High Order Rotor Vibration, American Helicopter Society 49th Annual Forum, St. Louis, Missouri, May 1993

Ref.8 *Langer, H.-J., Peterson, R.L., Maier, T.H.,* An Experimental Evaluation of Wind Tunnel Wall Correction Methods for Helicopter Performance, American Helicopter Society 52nd Annual Forum, Washington D.C., June 1996

Ref.9 *Schneider, O., van der Wall, B.G.,* Final Analysis of HART II Blade Deflection Measurement, 29th European Rotorcraft Forum, Friedrichshafen, Germany, 2003

Ref.10 *van der Wall, B., Burley, C.L., Yu, Y.H , Richard, H., Pengel, K., Beaumier, P.*, The HART~II test - measurement of helicopter rotor wakes, Aerospace Science and Technology, Vol. 8, pp. 273-284, 2004

Ref.11 *Hounjet, M.H.L., Eussen, B.J.G.,* Outline and Application of the NLR Aeroelastic Simulation Method, ICAS-94-9.4.2, pp 1418–1441

Ref.12 *Eussen, B.J.G, Hounjet, M.H.L., Zwaan, R.J.,* Experiences in Aeroelastic Simulation Practices, Proceedings EUROMECH Colloquium 349, Goettingen, Germany, 1997

Ref.13 *Hounjet, M.H.L, Meijer, J.J.,* Evaluation of Elastomechanical and Aerodynamic Data Transfer Methods for Non-planar Configurations in Computational Aeroelastic Analysis, IFASSD 1995

Ref.14 *Pengel, K., Müller, R., van der Wall, B.G.,* Stereo Pattern Recognition – the Technique for Reliable Rotor Blade Deformation and Twist Measurements, AHS International Meeting on Advanced Rotorcraft Technology and Life Saving Activities, Utsunomiya, Tochigi, Japan, 2002